ELSEVIER

Journal of Nuclear Materials 251 (1997) 172–187

journal of nuclear materials

Segregation of cascade induced interstitial loops at dislocations: possible effect on initiation of plastic deformation

H. Trinkaus [a,*], B.N. Singh [b], A.J.E. Foreman [c]

[a] *Institut für Festkörperforschung, Forschungszentrum Jülich, D-52425 Jülich, Germany*
[b] *Materials Research Department, Risø National Laboratory, DK-4000 Roskilde, Denmark*
[c] *Materials Performance Department, Harwell Laboratory, Oxfordshire OX11 0RA, UK*

Abstract

In metals and alloys subjected to cascade damage dislocations are frequently found to be decorated with a high density of small clusters of self-interstitial atoms (SIAs) in the form of dislocation loops. In the present paper it is shown that this effect may be attributed to the glide and trapping of SIA loops, produced directly in cascades (rather than to the enhanced agglomeration of single SIAs), in the strain field of the dislocations. The conditions for the accumulation of glissile SIA loops near dislocations as well as the dose and temperature dependencies of this phenomenon are discussed. It is suggested that the decoration of dislocations with loops may play a key role in radiation hardening subjected to cascade damage. It is shown, for example, that the increase in the upper yield stress followed by a yield drop and plastic instability in metals and alloys subjected to cascade damage cannot be rationalized in terms of conventional dispersed barrier hardening (DBH) but may be understood in terms of cascade induced source hardening (CISH) in which the dislocations are considered to be locked by the loops decorating them. Estimates for the stress necessary to pull a dislocation away from its loop 'cloud' are used to discuss the dose and temperature dependence of plastic flow initiation. © 1997 Elsevier Science B.V.

1. Introduction

It is now well established by experimental (for reviews see Refs. [1–3]) as well as molecular dynamics (MD) studies [4–7] that in displacement cascades vacancies and self-interstitial atoms (SIAs) are produced in a highly localized and segregated fashion resulting in efficient intracascade clustering of both types of defects. Small SIA clusters in the form of dislocation loops (coupled crowdions) have been found in MD studies to be highly mobile [6]. Such a loop may perform a thermally activated random glide motion by which it may leave its native cascade region and migrate over large distances until it interacts with another defect [1,2].

The recognition of intracascade SIA clustering ('production bias' [8,9]) in conjunction with the glide of small SIA loops provides an explanation for some specific microstructural features occurring under cascade damage conditions which cannot be treated in terms of the conventional rate theory approach based on single defect reaction kinetics [10,11]: (1) substantial void nucleation and growth at very low doses ($< 10^{-2}$ dpa), even without the assistance of helium, and at very low dislocation densities [12], and (2) an extremely non-homogeneous microstructural evolution at low doses with a pronounced segregation of SIA and vacancy components [12]. One example for the latter class of features is the enhanced swelling in several μm wide regions adjacent to grain and subgrain boundaries [13–15] (for further references see Refs. [1,2,16]). Other examples are the formation of patches or 'rafts' of dislocation loops [13,17–23] and the decoration of edge dislocations by loops [13,23–28] which may even extend to form dislocation walls [13,28–30]. In the present paper, interest will be focused on the decoration of dislocations with SIA loops.

Under electron irradiation, dislocations have been found occasionally to be decorated with stacking fault tetrahedra [31–33]. Accumulation of SIA loops near dislocations, on the other hand, seems to be a specific feature observed

* Corresponding author. Tel.: +49-2461 616 460; fax: +49-2461 612 620.

PII S0022-3115(97)00246-8

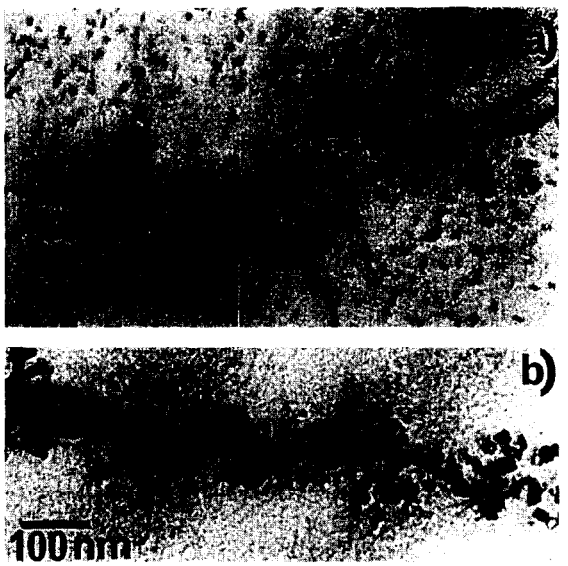

Fig. 1. Comparison between electron and neutron irradiation. (a) An electron micrograph showing the absence of dislocation decoration in a thin foil of Ni–0.3 at.% Ge irradiated with 1 MeV electrons at 473 K to a fluence level of 3.6×10^{25} e/m^2 (0.2 dpa) [27]. (b) A dislocation line heavily decorated with interstitial loops in Ni–2 at.% Ge (bulk) irradiated with 14 MeV neutrons at 563 K to a fluence level of 6×10^{22} n/m^2 (2×10^{-2} dpa) [27].

only under cascade damage conditions. This is illustrated in Fig. 1 where the features evolving in two almost identical NiGe alloys under electron and neutron irradiation are compared [27]. The electron micrograph of Fig. 1(a) shows a complete absence of dislocation decoration in Ni–0.3% Ge irradiated with 1 MeV electrons. In the case of neutron irradiated Ni–0.2% Ge shown in Fig. 1(b), on the other hand, a large number of dislocation loops are formed at or in the vicinity of a grown-in dislocation. Similar features have been observed in pure Ni [22,25], other Ni alloys [25], pure Cu and Cu alloys [26] as well as in pure Mo [23] and Mo alloys [17–23]. In pure copper, continuing decoration of dislocations with SIA loops under cascade damage conditions results in the formation of 'dislocation walls' even at doses below 10^{-2} dpa [13,28–30]. An example of wall formation in neutron irradiated Cu is shown in Fig. 2.

Pronounced microstructural features such as heavily decorated dislocations are expected to modify substantially the deformation behaviour since they would make the dislocation generation and hence the initiation of plastic flow difficult. In fact, the deformation characteristics of metals and alloys exhibiting dislocation decoration change qualitatively by cascade damage: thus, the yield stress increases with dose without dislocation generation and above some critical dose (≥ 0.01 dpa) the initiation of plastic deformation is associated with a prominent yield drop [28,34–38]. Beyond the yield drop, plastic deformation is localized in narrow bands commonly known as cleared channels containing practically no defect clusters. Frequently plastic instability [35–37] rather than work hardening is observed. This deformation behaviour is illustrated in Fig. 3 showing stress strain curves for polycrystalline pure copper neutron irradiated at 320 K [34] and for a Mo–Re alloy irradiated with 600 MeV protons at 310 K [36].

Since in the cases quoted above the accumulation of SIA loops near dislocations continues with irradiation dose even when the dislocations are already locked the decoration process must be considered to be due to SIA transport to the dislocations rather than to dislocation sweeping of SIA loops as assumed by Makin [39]. For SIA transport to and accumulation near a dislocation two possible mechanisms are conceivable: (a) the three-dimensional migration and enhanced agglomeration of single SIAs in the form of loops in the strain field of the dislocation, or (b) the glide and trapping of small SIA loops, directly produced in cascades.

Both of these possibilities have been examined recently [40]. Calculations have shown [40] that the strain field of a dislocation with an edge component causes a SIA depletion in the compressive as well as in the dilatational region resulting in a reduced rather than enhanced agglomeration of SIAs in the vicinity of a dislocation (whereas SIA depletion may induce enhanced vacancy agglomeration). It

Fig. 2. An example of dislocation wall formation in pure copper irradiated with fission neutrons at 523 K [28] to a fluence level of 5×10^{22} n/m^2 (10^{-2} dpa, $E>1$ MeV) [28].

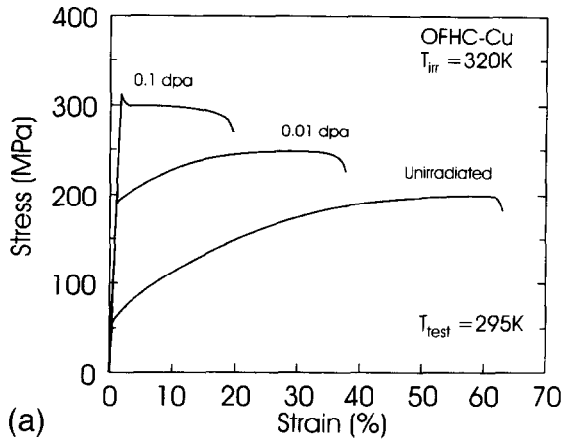

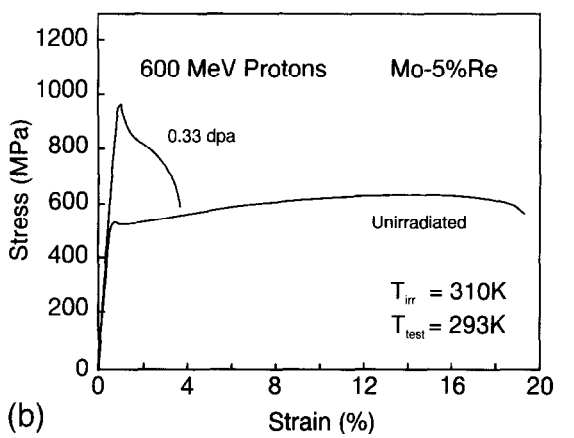

Fig. 3. Stress–strain curves for (a) pure polycrystalline copper irradiated with fission neutrons at 320 K [34], (b) Mo–5% Re alloy irradiated with 600 MeV protons at 310 K [36]. Note the yield drop and lack of work hardening in both cases.

has been argued, on the other hand, that the second mechanism, i.e., the trapping of glissile loops in the strain field of the dislocation, can easily account for the decoration phenomenon. In the first part of the present paper (Section 2), these considerations are reviewed and the discussion of SIA loops accumulation near dislocations in terms of glissile loop trapping is extended, particularly concerning the conditions for this mechanism to be operative and its dose and temperature dependencies.

Recently it has been argued [41] that the increase in the observed upper yield stress followed by a yield drop and plastic instability in metals and alloys subjected to cascade damage cannot be rationalized in terms of conventional dispersed barrier hardening (DBH) [42–45] in which a dispersed distribution of rigid and indestructible obstacles is assumed to act against the dislocation motion. It has been proposed [41] to explain these features of radiation hardening in terms of cascade induced source hardening (CISH) by SIA loops decorating the grown-in dislocations. The mechanism of 'source hardening' due to 'clouds of defects' along the dislocations was suggested many years ago [46–49]. However, in these early works, neither the nature of the clouds of defects nor the mechanism of their formation were identified. In the CISH model the upper yield stress in the irradiated materials is determined by the stress necessary to pull the grown-in dislocations from the clouds of small SIA loops around them. In the second part of the present paper (Section 3), the model suggested for the decoration of dislocations by glissile loops is applied to CISH to estimate the upper yield stress. Finally, the physical basis for the dose and temperature dependencies of the upper yield stress expected from the CISH model is discussed.

2. Mechanisms for decoration of dislocations by small loops

The microstructural evolution during irradiation is controlled by the interaction among the irradiation-induced primary defects and the interaction of these defects with the existing extended defects such as voids and dislocations. The accumulation of defects in the vicinity of a dislocation requires a long-range interaction mediated by stress/strain fields of the defects involved. In order to carry out the following analyses it is useful to reconsider the basic features of this elastic interaction.

2.1. Elastic interaction between a dislocation and point defects and their clusters

For distances that are large compared to the dislocation core radius and the defect size, the interaction of a defect with the stress field $\sigma(r)$ of a dislocation may be described by the elastic dipole approximation as [50]

$$E(\boldsymbol{r}) = -\mathbf{Q}\boldsymbol{\sigma}(\boldsymbol{r}), \quad \text{with trace}\,\mathbf{Q} = \Delta V, \tag{1}$$

where $\mathbf{Q}$ is the strain tensor and ΔV is the relaxation volume of the defect. A possible difference between $\mathbf{Q}$ and ΔV values in equilibrium and saddle point positions will be ignored in the following treatment for the sake of simplicity. Since $\boldsymbol{\sigma}(-\boldsymbol{r}) = -\boldsymbol{\sigma}(\boldsymbol{r})$, the angular dependence of the interaction energy is characterized by attractive and repulsive directions with a vanishing directional average (see Fig. 4). Otherwise the angular dependence of $E(\boldsymbol{r})$ is complicated and closed analytical expressions exist only for the case of elastic isotropy. For single SIAs and vacancies we assume in addition that $\mathbf{Q}$ is isotropic. In this case, the energy of a defect of relaxation volume ΔV in the strain field of an edge dislocation of Burgers vector b may be written as [50]

$$E(r) = p\Delta V = -(A\cos\varphi)/r$$
$$\text{with } A = \frac{1}{3\pi}\frac{1+\nu}{1-\nu}\mu\Delta V b, \tag{2}$$

where r is the distance between the defect and the dislocation, φ is the angle between the distance vector and the direction of maximum dilation (see Fig. 4), ν is Poisson's ratio and μ is the shear modulus of the medium. The equipotential lines are double-circles (double-cylinders) as shown in Fig. 4. Assuming $\nu = 1/3$ and $\mu\Omega \approx 35kT_m$ [1,2], the constant A in Eq. (2) is estimated to scale as $7kT_m b\Delta V/\Omega$, where Ω is the atomic volume and T_m is the melting temperature. With this, the effective trapping radius below which the magnitude of the (maximum) attractive interaction is larger than the thermal energy kT may be estimated as $r_t = A/kT = 7(T_m/T)(\Delta V/\Omega)b \approx 20b$ for $T = 0.35T_m$ and $\Delta V = \Omega$.

In the present context, the difference between the values of ΔV for SIAs and vacancies in metals is important. The relative volume change $\Delta V/\Omega$ is positive for SIAs with values between 1 and 2, whereas it is negative for vacancies with values between -0.05 and -0.25 [51]. Thus, according to Eq. (2), the interaction is not only opposite (and attractive in opposite directions) but also considerably weaker (by an order of magnitude) for vacancies than for SIAs.

As for single point defects, the elastic dipole approximation for the interaction of a small loop with the stress field of another defect such as a dislocation is given by Eq. (1) (infinitesimal loop approximation). For a loop, the strain tensor is, however, clearly anisotropic. For complete relaxation (large loops), $\mathbf{Q}$ may be written in the form

$$Q_{kl} = A_k b_l, \quad \text{with } \boldsymbol{A} \cdot \boldsymbol{b} = A_k b_k \approx n\Omega, \tag{3}$$

where $\boldsymbol{A}$ is the area vector of the loop, $\boldsymbol{b}$ is its Burgers vector (BV) and n is the number of single defects (SIAs) in the loop. The corresponding equipotential lines are more complicated than for isotropic $\mathbf{Q}$ and depend on the configuration of the loop relative to the dislocation as illustrated in Fig. 5 for the interaction of three perfect loop configurations with a perfect edge dislocation in an elastically isotropic fcc crystal. The interaction is strongest for parallel BVs. With $\mu\Omega = 35kT_m$ [1,2] an upper bound estimate of the interaction energy may be written as

$$|E| \le 0.35\mu\Omega n/r \approx 12bnkT_m/r, \tag{4a}$$

$$|E| \ge kT \quad \text{for } r \le 12bnT_m/T. \tag{4b}$$

According to Eq. (4b) a maximum range r as high as 90 nm is estimated for $b = 0.25$ nm, $n = 10$ and $T = T_m/3$. We emphasize here that the upper bound estimates for the interaction energy and the range where its magnitude is larger than kT as given by Eq. (4a) are meant for the most strongly interacting dislocation/loop configuration (both of edge type, parallel BVs) and are thus substantially higher than the estimates for the 'average interaction' given in Refs. [1,2].

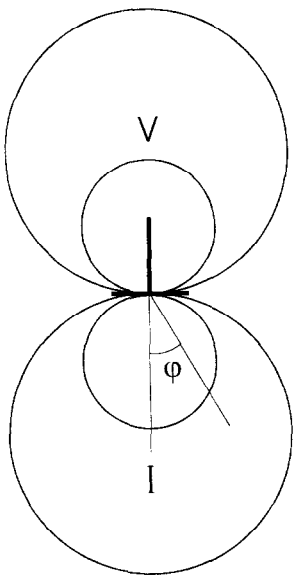

Fig. 4. Equipotential lines for the interaction of a point defect with an edge dislocation in an elastically isotropic medium. Regions favoured by SIAs and vacancies are indicated by I and V, respectively.

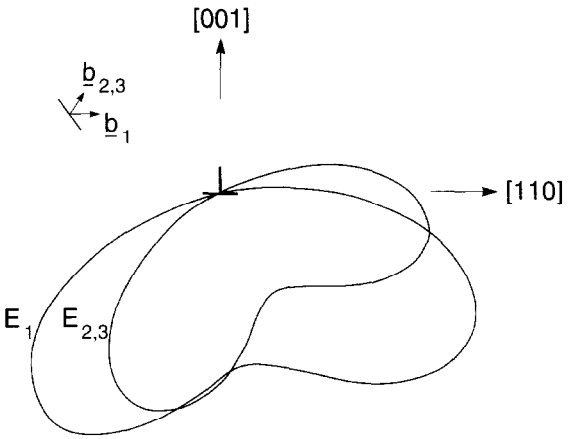

Fig. 5. Equipotential lines, $E(r)$ constant in the $(1\bar{1}0)$-plane for the interaction between a perfect edge dislocation with Burgers vector $[110]/2$ along the $[1\bar{1}0]$ direction and perfect SIA loops with Burgers vectors $\boldsymbol{b}_1 = [110]/2$, $\boldsymbol{b}_2 = [011]/2$, $\boldsymbol{b}_3 = [101]/2$ on (111)-planes in an elastically isotropic fcc crystal. b_2 and b_3 have equal components in and opposite components perpendicular to the $(1\bar{1}0)$-plane, respectively, and $E_2 = E_3$. From the attractive part shown the repulsive part is obtained by inversion. The contours for the interaction with loops on $(11\bar{1})$-planes are obtained by reflection on the (110) plane. The interactions for the other 6 loop configurations on $(1\bar{1}1)$- and $(\bar{1}11)$-planes are substantially weaker (narrower contours).

2.2. Would single SIAs and vacancies accumulate near dislocations?

While explaining the irradiation induced decoration of dislocations with small SIA clusters, it is frequently argued that the nucleation and growth of such clusters would be

favoured in the region of positive dilatational strain in the neighbourhood of a dislocation where the elastic interaction between the dislocation and the SIAs is attractive [24]. This possibility including its counterpart, i.e., the possibility of enhanced vacancy agglomeration will be examined in the following section.

The formation of clusters of a certain type of defect (SIA or vacancy) depends crucially upon the respective defect concentration which in turn is controlled by the balance of defect production, transport and annihilation. This holds globally for the cluster evolution on a large scale as well as locally on smaller (mesoscopic) scales. Thus, the defect concentrations near dislocations are determined by the defect fluxes in the elastic strain field induced by the dislocations. Neglecting here, for simplicity, possible differences between the interactions in the equilibrium and saddle point configurations we may write the flux density of a defect as [52]

$$\boldsymbol{j}(\boldsymbol{r}) = -D\exp(-\beta E(\boldsymbol{r}))\nabla\exp(+\beta E(\boldsymbol{r}))c(\boldsymbol{r}),$$
$$\text{with } \beta = 1/kT, \tag{5}$$

where D is the diffusion coefficient and $c(r)$ is the concentration of the defect. (Since SIAs and vacancies are treated analogously the defect types are not labeled here.)

An efficient segregation of defects near a dislocation requires defect transport into this region implying that the width of this region is small compared to the overall diffusional mean free path. For discussing the conditions for defect segregation there, it is sufficient to consider the initial stage of this process where quasi-steady state of the single defects is already established but cluster formation is still negligible. Under these conditions, defect conservation may be expressed by

$$\operatorname{div}\boldsymbol{j}(\boldsymbol{r}) = 0. \tag{6}$$

In general, solutions of Eq. (6) together with Eq. (5) are complicated because of the complicated angular dependence of $E(\boldsymbol{r})$ (see Fig. 5). Useful analytical solutions are, however, available for isotropic $\mathbf{Q}$ where $E(\boldsymbol{r})$ is given by Eq. (2) [53,54].

For solving Eq. (6) together with Eqs. (2) and (5) the boundary conditions must be specified. Considering the dislocation to be a perfect sink for SIAs and vacancies, we may assume the defects to be in local equilibrium close to the dislocation core, $r \to r_0$, i.e.,

$$c(\boldsymbol{r}) \to c^{\mathrm{eq}}(\boldsymbol{r}) = c_\infty^{\mathrm{eq}}\,\mathrm{e}^{-\beta E(r)} \quad \text{for } r \to r_0, \tag{7}$$

where c_∞^{eq} is the equilibrium concentration far from the dislocation. The angular variation of $c^{\mathrm{eq}}(\boldsymbol{r})$ may become extremely large for $r \to r_0$ and its maximum value may substantially exceed c_∞^{eq}, particularly for SIAs where ΔV is large. On the other hand, the values of c_∞^{eq} are negligible compared to typical values for irradiation induced defect concentrations in the temperature range of interest ($T < 0.5T_{\mathrm{m}}$). For defect agglomeration, the differences with respect to the local equilibrium concentrations are relevant.

Since we are interested in defect accumulation in the region $r_0 \ll r < r_{\mathrm{t}}$, we may set $r_0 \to 0$. Thus, we may use the boundary condition

$$\Delta c(\boldsymbol{r}) = c(\boldsymbol{r}) - c^{\mathrm{eq}}(\boldsymbol{r}) \to 0 \quad \text{for } r \to 0. \tag{8}$$

Since this boundary condition keeps the excess defect concentrations low close to the dislocation, enhanced defect agglomeration can only be expected in an intermediate range not too close to ($r \gg r_0$) and not too far from the dislocation ($r < r_{\mathrm{t}}$). For large r where $\Delta c(\boldsymbol{r})$ becomes independent of the direction an appropriate embedding procedure is needed. With boundary condition (8) for $r_0 \to 0$, the complicated general solution [54] for Eq. (6) together with Eqs. (2) and (5) simplifies to [53]

$$\Delta c(\boldsymbol{r}) = CF(\boldsymbol{r}),$$
$$\text{with } F(\boldsymbol{r}) = (2\pi)^{-1}\exp[\beta A(\cos\varphi)/2r]K_0(\beta A/2r), \tag{9}$$

where K_0 is the modified Bessel function of zero order and C is an integration constant to be determined by the embedding procedure. For sink controlled defect annihilation, for instance, this may be done by considering an appropriately weighted partitioning of the defects over the available sinks. Thus, the total defect flux per unit length to one dislocation, is defined by the behaviour of Eq. (9) for $r \to \infty$ as $I = 2\pi rj(r \to \infty) = DC$, which must be equal to the defect production rate, P, per overall sink strength, k^2. Hence

$$C = P/Dk^2, \tag{10}$$

where a biased absorption of the defects by sinks is neglected.

In Fig. 6, the spatial dependence of the excess concentration near a dislocation is illustrated in plots of $F(r)$ vs. r as given by Eq. (9) for the directions of maximum

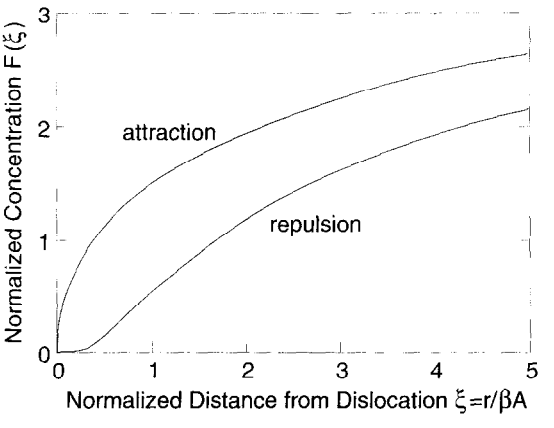

Fig. 6. Normalized (excess) defect concentration, $(Dk^2/P)\Delta c = F(\xi)$ vs. normalized distance from the dislocation, $\xi = r/\beta A$, for maximum attraction and repulsion, respectively, according to Eq. (9).

attraction and repulsion ($\varphi = 0$ and $\varphi = \pi$ for SIAs), respectively. Fig. 6 shows clearly that even on the attractive side the defect concentration decreases monotonically with decreasing distance from the dislocation — opposite to what one could expect intuitively. This decrease occurs inspite of the decrease of the effective cross-section for the defect flux with decreasing distance from the dislocation, an (thus invalid) argument for enhanced SIA accumulation used by Kiritani [24].

The reduction of the (excess) concentration of each type of point defect everywhere close to the dislocation even on the corresponding attractive side is, however, not sufficient to rule out enhanced agglomeration of one or the other type of cluster since the nucleation and growth of such clusters is controlled by the *difference* in the absorption of SIAs and vacancies rather than by the absorption of just one of these two types of defects. Thus, a strong depletion of defects of one type at the side where their interaction with the dislocation is repulsive could favour the clustering of defects of the opposite type which feel an attractive interaction there. Because of the small magnitude of the relaxation volume of vacancies as compared to SIAs, substantial vacancy depletion in the dilatational region of the dislocation is, however, restricted to such a narrow region close to the dislocation that it cannot account for the observed SIA accumulation there [40]. On the other hand, the much wider SIA depletion in the compressive region may induce enhanced vacancy agglomeration there which would explain the occasionally observed decoration of dislocations with stacking fault tetrahedra under electron irradiation [31–33].

For the accumulation of SIAs in the form of clusters near dislocations we may conclude that this phenomenon cannot be rationalized in terms of the production, three-dimensional diffusion and enhanced agglomeration of single SIAs — at least as long as the dislocations may be considered to be good sinks for SIAs and vacancies. This holds, however, even in the unlikely case of dislocations blocked by closed rows of impurities along their cores [40]. In this case, the SIA concentration and even more strongly the SIA clustering rate would indeed be enhanced in the dilatational region as soon as quasi-steady state is established. The SIA precipitation at the core of the original dislocation would, however, readily lead to a reconstruction of a new clean dislocation suppressing further SIA clustering as discussed above.

So far, we have assumed that the diffusion of the single SIAs is three-dimensional and concluded that, in this case, no enhanced SIA clustering would occur near dislocations. In the present context, we should, however, also consider the possibility of SIAs produced in the crowdion configuration which would be constrained to one dimension and thus could be trapped by a dislocation without getting absorbed by it. There is, however, general consensus that in the strong distortion field of a dislocation crowdions, even if they were metastable in the undistorted lattice, would readily convert to the three-dimensionally migrating dumb-bell configuration which would annihilate at the dislocation. In the following section, we shall, however, consider the possibility of a one-dimensional migration of defect clusters produced as coupled crowdions in the form of perfect loops [6,7].

We may summarize this section by stating that the observed segregation of SIA loops near dislocations is unlikely to be due to a preferential clustering of single SIAs there.

2.3. Accumulation of glissile loops near dislocations

There is now plenty of direct and indirect evidence from experimental and molecular dynamics studies that in displacement cascades a substantial fraction of SIAs are produced in the form of clusters and that some of these clusters are glissile [1–7]. Such a loop may perform a thermally activated random glide motion until it gets trapped in the strain field of another defect cluster or a dislocation. In pure metals, small glissile loops are expected to be highly mobile. Impurities will reduce their mobility by binding them temporarily [2,3]. It should be noticed here that, in contrast to small SIA loops, small vacancy loops are not known to be glissile [2].

There are two important aspects in the kinetics of one-dimensionally migrating defects in comparison to the kinetics of three-dimensionally migrating defects: (1) the range of free migration and (2) the impeded absorption once the defect is trapped in the strain field of another defect. The crucial quantity characterizing the range of a one-dimensionally migrating defect is its mean free path. For a defect of configuration i migrating one-dimensionally in a crystal containing a number density c_j of immobile defects of configuration j with effective interaction cross-section $\sigma_{ij} = \pi r_{ij}^2$ and a line density ρ of dislocations with effective interaction diameter d_i the reciprocal mean free path $\kappa_i = \lambda_i^{-1}$ is given by [1,2]

$$\kappa_i = \lambda_i^{-1} = \Sigma_j \sigma_{ij} c_j + d_i \hat{\rho}, \tag{11}$$

where $\hat{\rho} = \pi\rho/4$ is the dislocation line length per unit volume projected on a plane perpendicular to the migration direction. σ_{ij} and d_i are the cross-sections and diameters of the regions where defects i are more likely to be annihilated than be detrapped (see below). The sink strength for the annihilation of defects i is given by κ_i^2 [1–3].

The most important feature of Eq. (11) is that, for low and moderate defect densities, c_i, ρ, the ranges of small glissile loops are of the order of several μm and are thus significantly larger than for three-dimensionally migrating point defects. Consequently, the microstructural evolution occurs, particularly at low doses and in well annealed pure metals, in a very heterogeneous fashion characterized by a large-scale segregation of SIA-type and vacancy type defects. Under such conditions, a grown-in dislocation would

have a large drainage area for accumulating glissile loops in its neighbourhood.

Generally, a glissile loop is trapped in a metastable state near a dislocation — unless it encounters the dislocation while it is gliding. Absorption of a trapped loop into the dislocation requires a change in the direction of motion of the loop either by a thermally activated BV change or by conservative ('self') climb via core diffusion, or a mutual approach of the loop and the dislocation by a joint motion in the case of non-parallel BVs as shown schematically in Fig. 7. In the latter case, the loop would be readily absorbed. This requires, however, that the dislocation is glissile and its motion is not yet impeded. (For further details in loop absorption see below.)

The details in the approach of a (single) glissile loop to a (non-decorated) dislocation are rather complicated as illustrated in Fig. 8 where the paths of loops followed by combined climb and glide along the valleys and by zigzag glide with BV changes in metastable positions, respectively, are shown for the loop/dislocation configurations considered in Fig. 5. The tangential points of the paths with the corresponding equipotential lines give the locations of potential energy extreme. For each configuration, the set of relative minima defines the two valley floors separated by a mountain ridge. If climb dominated over BV changes, a loop would move down a valley by combined climb and glide. If BV changes dominated over climb, a loop would change between neighbouring valleys V_1 and $V_{2,3}$ in a zigzag motion. Note that a BV change from $\boldsymbol{b}_{2,3}$ to $\boldsymbol{b}_1$ would be facilitated by an associated decrease in the interaction potential whereas a BV change from $\boldsymbol{b}_1$ to $\boldsymbol{b}_{2,3}$ would be rendered more difficult by an increase in the interaction potential. In the general case, the loop paths to the dislocation would be between the extreme cases shown in Fig. 8. Note that the less strongly interacting loops on $(1\bar{1}1)$ and $(\bar{1}11)$ planes cannot reach the dislocation by alternating BV changes since in this case a glide motion parallel to the dislocation is involved.

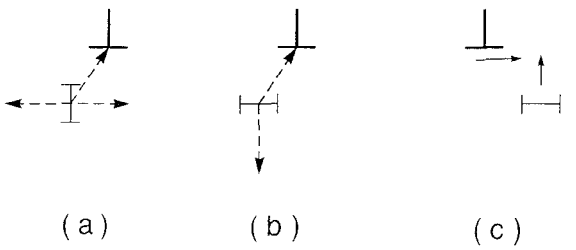

Fig. 7. Possible configurations for the trapping and absorption of a glissile loop by a dislocation segment, (a) metastable trapping state for parallel Burgers vectors, (b) metastable trapping state at a sessile dislocation segment for nonparallel Burgers vectors, (c) absorption of a loop by a joint motion with a glissile dislocation segment. In cases (a) and (b), absorption requires Burgers vector

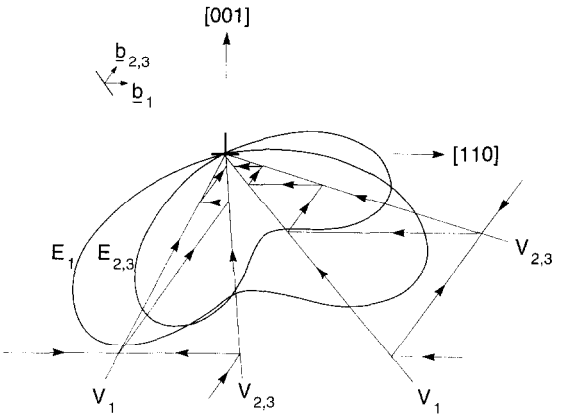

Fig. 8. Paths of glissile loops for approaching a dislocation by combined climb and glide along the valleys $V_{1,2,3}$ and by zigzag glide with BV changes in metastable valley positions, respectively, for the loop/dislocation configurations considered in Fig. 5.

The approach of a loop to a dislocation as suggested in Fig. 8 is, however, restricted to a region sufficiently close to the dislocation but not so close such that, on one hand, diffusion in the loop motion is negligible against drift, and, on the other hand, the elastic continuum approach in general and the 'infinitesimal loop approximation' in particular are still applicable. In fact, the details of the fate of a loop approaching a dislocation depends, via the magnitude of the interaction energy, on the distance from the dislocation as schematically illustrated in Fig. 9 (assuming a simplified interaction potential as in Fig. 4). In the region 1 far away from the dislocation where $|E(r)| < kT$ the loop is expected to perform a thermally activated random glide motion. In the outer part of the trapping region (region 2) where $|E(r)| > kT$, thermally activated detrapping will dominate but the interaction with other loops or even loop agglomeration in this region may impede detrapping since loop complexes are more strongly bound to the dislocation than single loops. At distances somewhat closer to the dislocation (region 3), thermally activated BV changes and/or conservative climb will dominate over detrapping. As a loop approaches the dislocation even closer, the barrier against BV changes or climb may disappear and the motion may become unstable (region 4). When the loop comes very close (i.e., within a few b) to the dislocation (innermost region 5) it may disintegrate in a kind of melting process and get incorporated into the dislocation. The situation becomes more complicated when trapped loops begin to interact.

The density of loops accumulated in the neighbourhood of a dislocation will depend on the loop arrival rate determined by production rate of glissile loops in cascades and the loop trap (dislocation) density. For low loop arrival rates (low loop production rate/high trap density) loop

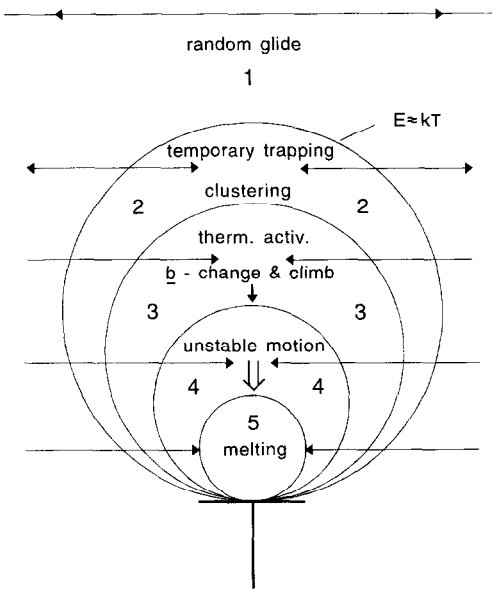

Fig. 9. Sketch of characteristic regions in the interaction of a glissile interstitial loop with an edge dislocation. In region 1 where $|E| \leq kT$, a glissile loop performs a virtually free thermally activated one-dimensional random walk motion. In regions 2–5 where $|E| \geq kT$, the motion of the loop is significantly affected by the interaction with the dislocation. In region 2, thermally activated detrapping dominates over changes in the direction of motion of the loop but the interaction with other loops or even loop clustering may impede detrapping. In region 3, thermally activated BV changes and/or conservative climb dominate. In region 4, the loop motion becomes unstable and, in region 5, the loop disintegrates and gets incorporated into the dislocation.

the outer boundary of the region where BV changes and climb become dominant (region 3) defines the loop absorption range of the dislocation. For high loop arrival rates (high loop production rate/low trap density), loop interaction will reduce the detrapping rate as well as the rate of BV change and climb. In addition, loops may become sessile by faulting. These processes will lead to an accumulation of loops in the corresponding regions (regions 2 and 3). Thus, for the limiting case of very high loop arrival rates, the initial extension of the region of decoration is given by the boundary of the trapping region (90 nm in the above example). Virtually no loop accumulation will occur in the inner regions of rapid unstable approach (4 and 5) where the loop density is expected to remain very low.

Several characteristic phases of the decoration process may be distinguished as shown schematically in Fig. 10. In the first phase, loop trapping in the region of strong attractive interaction occurs resulting in loop accumulation inspite of partial detrapping and absorption; mutual immobilization of loops, loop agglomeration and growth (coarsening) are still negligible; quasi-equilibrium concentration (Cottrell cloud) and quasi-steady state concentrations of loops are established in regions 2 and 3 of Fig. 9, respectively. The second phase is characterized by loop agglomeration and growth under continued loop trapping; a repulsive force against further loop trapping gradually builds up. In the third phase, loop trapping ceases and the SIA content in the primary trapping region saturates since the attractive stress field of the leading dislocation is now fully compensated by already existing loops. Concerning the stress field, the whole dislocation/loop configuration is equivalent to a dislocation shifted by the extension of the primary region of loop trapping. Loop trapping occurs now only ahead of the existing structure where the elastic interaction remains attractive. Accordingly, the structure grows by further loop trapping in the direction where the interaction is strongest, i.e., away from the leading dislocation, and begins to form a dislocation wall there. In a possible late fourth phase the supply of glissile loops may exhaust due to the overall build up of the microstructure. In such a late phase, loop absorption by the dislocation may result in a shrinkage or even disappearance of the pronounced structures occurring in the third phase.

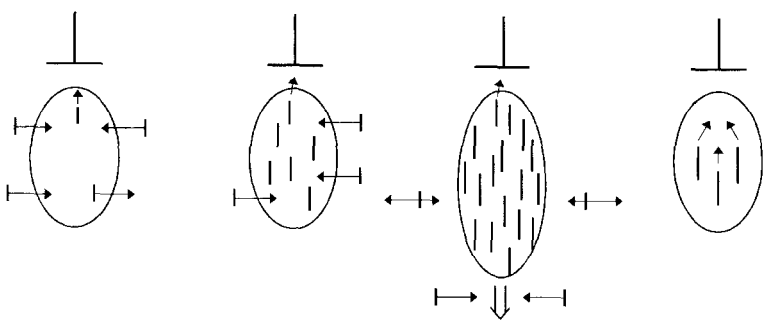

Fig. 10. Sketch of characteristic phases in the decoration of dislocations with loops: (1) loop accumulation by trapping in region of strong attractive interaction inspite of partial detrapping and absorption; loop clustering negligible; loop accumulation until quasi-equilibrium/quasi-steady state is reached; (2) loop clustering and growth (coarsening) under continued trapping; building up of repulsive counter force field; (3) end of loop trapping and saturation of SIA content in the primary region of loop accumulation; growth of the structure by loop trapping away from the dislocation resulting in wall formation; (4) exhaustion of loop supply due to the overall build up of the microstructure; coarsening, shrinkage and disappearance of the loop structure.

So far, we have ignored the influence of point defects on the decoration process. We restrict ourselves here to emphasizing one important fact: because of strong competition, clusters densely arranged along dislocations are much less sensitive to point defect absorption than those between the dislocations.

2.4. Evaluation of conditions for loop accumulation

A necessary condition for an undelayed and pronounced accumulation of glissile loops near dislocations is that the trapping of a single loop in the strain field of a dislocation is not terminated by detrapping or BV change or substantially disturbed by climb before it is immobilized by another loop trapped in its neighbourhood. This implies that the region 2 in Fig. 10 is sufficiently large or the region 3 sufficiently small. To quantify this condition the characteristic times for detrapping, BV change, climb and loop agglomeration must be discussed in terms of their relation to each other and as a function of the distance to the dislocation.

The supply of glissile loops to the strain field of a dislocation is controlled by their production and annihilation in the environment of the dislocation. Steady state may be expressed by

$$P_g = D_g \bar{c}_g \kappa^2, \tag{12}$$

where P_g is the production rate, D_g the one-dimensional diffusion coefficient for random glide and $\bar{c}_g$ the average concentration of glissile loops, and κ^2 is the total sink strength according to Eq. (11) for their annihilation in the environment of the dislocation. Note that Eq. (12) holds separately for all equivalent loop configuration with equal $\kappa_i \equiv \kappa$ as given by Eq. (11). P_g may be related to the NRT displacement rate G (in dpa/s) via [1–3]

$$P_g = \varepsilon_i^g G / n_i^g \Omega, \tag{13}$$

where ε_i^g is the fraction of SIAs produced in the form of glissile loops (including direct production in cascades as well as contributions form sessile–glissile loop transformation [3]) and n_i^g is the average number of SIAs per glissile loop.

The characteristic time of trapping or detrapping, τ_t, may be estimated in the following way. Consider a cylindrical region with its axis parallel to the glide direction of a certain glissile loop configuration g' and with a cross-section σ and a length corresponding to the effective width w of the potential energy minimum ('valley') in the strain field of the dislocation. Note that w scales with the distance from the dislocation, r. The number of loops N' of configuration g' flowing per unit time from one side through the cross-section into the valley is given by

$$\mathrm{d}N'/\mathrm{d}t = D_g \bar{c}'_g \kappa \sigma. \tag{14}$$

If neither BV change nor climb occurred, the equilibrium would be established when the loop fluxes into and out of the valley would balance each other. In this state, the number of loops of configuration g' in the cylinder of volume $\sigma w \approx \sigma r$, N'_{eq}, may be approximated by

$$N'_{eq} \approx \sigma r \bar{c}'_g \exp(-\beta E(r)), \tag{15}$$

where $E(r)$ is the (negative) minimum energy along the coordinate of the loop path. Eqs. (14) and (15) yield an estimate for the trapping/detrapping time according to

$$\tau_t \approx N'_{eq}/(\mathrm{d}N'/\mathrm{d}t) \approx (r\lambda/D_g)\exp(-\beta E(r)). \tag{16}$$

Assuming that BV changes of small glissile loops occur by thermal activation we describe the average time between two BV changes by an Arrhenius behaviour

$$\tau_b = \tau_0 \exp(\beta E_b), \tag{17}$$

where the pre-exponential term τ_0 is estimated to be of the order of 10^{-13} s. Unfortunately, not much is known about the activation energy E_b. In MD studies of cascade defects in Cu, the change in the BV of a cluster consisting of four SIAs ('coupled crowdions') has been observed [6]. From the lifetime of a given configuration a relatively low value of 0.4 eV has been estimated for the barrier against this transformation. This estimate is, however, rather uncertain because of the lack of statistics. E_b certainly increases with increasing loop size and would be proportional to $n_i^{1/2}$ if the BV changes were controlled by the sweeping of a partial dislocation across the loop area.

To estimate the time required for a loop to reach the dislocation by climb, τ_c, we consider its drift velocity in the force field of the dislocation

$$\boldsymbol{v}(\boldsymbol{r}) = -\beta \mathbf{D}_c \nabla \boldsymbol{E}(\boldsymbol{r}), \tag{18}$$

where $\boldsymbol{D}_c$ is the (two-dimensional) diffusion tensor of the loop associated with climb. Below $0.5T_m$, the fastest climb mechanism is conservative 'self-climb' by dislocation core diffusion [55] the activation energy of which may be expected to be comparable with those for self-diffusion along dislocations and grain boundaries which are around $9kT_m$ [2]. This conservative loop climb is characterized by a loop diffusion coefficient, D_c, which is proportional to the dislocation core diffusion coefficient D_{dc} and decreases with increasing size n_i as $D_c \approx D_{dc}/n_i^{3/2}$. Using $v \approx r/\tau_c$ and $\beta \nabla \boldsymbol{E}(\boldsymbol{r}) = \beta E(r)/r$ we may estimate the time required for a loop to reach the dislocation as

$$\tau_c \approx r^2/3\beta E(r) D_c. \tag{19}$$

According to the above discussion, the transition from the dominance of detrapping to the dominance of BV change or climb (regions 2 and 3 in Fig. 9) is defined by $\tau_t(r) \approx \tau_{b,c}(r)$. The requirement of a pronounced trapping region 2 results in the condition $E_g < E_c < E_b$ (with some uncertainty related to the uncertainties in the pre-exponential factors in Eqs. (16), (17) and (19)). A more restrictive

condition is imposed by the requirement of mutual immobilization of loops by agglomeration.

The characteristic time for the arrival of a second loop in the interaction range of a loop trapped before, τ_i, may be estimated on the basis of Eq. (14) in conjunction with Eqs. (12) and (13) by interpreting σ in Eq. (14) as the effective loop–loop interaction cross-section and dN/dt as just one loop arriving in a time interval τ_i. Assuming the ratio of the geometrical cross-section $\pi r_1^2 = n\Omega/b$ to the interaction cross-section σ to be α we estimate τ_i as

$$\tau_i = \left(D_g c_g \kappa \sigma \right)^{-1} = \alpha b / \varepsilon_i^g G \lambda. \quad (20)$$

Eq. (20) is, of course, not restricted to the vicinity of the dislocation. Here, however, the (primary) concentration of glissile loops is substantially larger than in the regions remote from the dislocation. τ_i may be interpreted as an incubation time for the build up of the loop cloud (phase 1 and 2 in Fig. 10).

For the occurrence of an undelayed and pronounced decoration, each primary loop trapped in the strain field of a dislocation must be immobilized by agglomeration before it is detrapped or absorbed by the dislocation via BV change or climb. This requires that

$$(\tau_t, \tau_b, \tau_c) \geq \tau_i. \quad (21)$$

If these conditions were not fulfilled mutual loop immobilization would depend on chance, i.e., the probability of its occurrence would be below 1. If Eq. (21) were only weakly violated loop accumulation at dislocations could still take place even if delayed and less pronounced.

Since the decrease of τ_t, τ_b and τ_c with increasing temperature is stronger than that of τ_i, these conditions are most critical at the high temperature limit of the decoration phenomenon, i.e., around $0.4T_m$ in fcc metals. Assuming for this temperature $\lambda = 20$ μm for doses below 10^{-3} dpa (as suggested by experimental data reviewed in Ref. [16]), $G = 10^{-7}$/s, $\varepsilon_i^g = 5\%$ and $\alpha = 20\%$ (corresponding to loop distance $\approx 2 \times$ loop diameter) we estimate τ_i to be of the order of 500 s (5×10^{-5} dpa). Assuming in Eqs. (16), (17) and (19), definitive loop trapping at $r < 20$ nm, $\beta E(r) = -3$ (at 1/3 of the average trapping radius), pre-exponential factors of 10^{-6} m^2/s, 10^{-8} m^2/s and 10^{-13} s for D_g, D_c, and τ_0, respectively, we deduce from Eq. (21) the conditions $(E_g, E_b, E_{dc})/kT_m \geq 7.5$, 14 and 10, respectively. The lower bound value of 10 for E_{dc} is in approximate agreement with our previous assumption of 9, whereas the values for E_g and E_b are significantly higher than expected for small groups of crowdions [7], indicating that the glissile loops contributing to decoration at high temperatures around $0.4T_m$ may be substantially larger than such small clusters. A similar conclusion has been drawn in a different way in Ref. [40]. According to these estimates, single crowdions as well as small groups of them would be readily absorbed by the dislocation.

A possible mechanism by which both the high effective migration energy of glissile loops and the even higher activation energy for BV changes required for pronounced decoration at high temperature could be explained is sketched in Fig. 11. Each loop is assumed to be able to change by thermal activation from a stable sessile configuration to several equivalent metastable glissile configurations (3 in fcc crystals) separated from the sessile configuration by an energy ΔE. In this case, the effective energy for BV changes, E_b, would be identical with the sessile/glissile transformation energy. The effective diffusion energy of this migration mode, E_g^*, would be given by the sum of the energy difference, ΔE, and the migration energy of the glissile configurations, E_g, i.e., $E_g^* = \Delta E + E_g$. An increase in the effective glide diffusion energy would also be obtained by a binding of the loops to impurities. We emphasize here that the 'glissile' SIA loops responsible for dislocation decoration at high temperatures

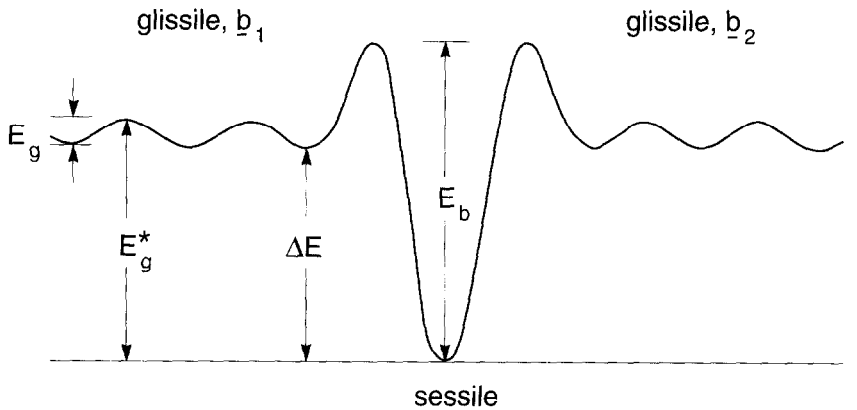

Fig. 11. Possible migration mode of loops: Thermally activated transformation of a stable sessile configuration with activation energy E_b into equivalent metastable glissile configurations separated from the sessile configuration by ΔE and diffusing with migration energy E_g. E_b is also the effective energy for Burgers vector changes. The effective diffusion energy of this mode is $E^* = \Delta E + E_g$.

need not necessarily originate directly from cascades but may result from reactions of cascade induced SIA clusters in the environment of the dislocation.

2.5. Temperature and dose dependencies of dislocation decoration

The activation energies controlling diffusion and BV changes of SIA loops must be considered to depend sensitively on their size. The wide temperature range (0.15 to $0.4T_m$) in which decoration of dislocations with loops occurs may be explained by a broad spectrum of SIA cluster sizes resulting from intra- and inter-cascade SIA clustering. At each temperature within this range, a certain set of sizes with activation energies appropriate for loop accumulation may be expected to be available. Thus, the loop size responsible for the nucleation of a dense loop structure will increase with temperature. At low temperatures, large loops will not contribute to the evolution of the loop structure because of their low mobility whereas at higher temperatures highly mobile small loops may still contribute to the growth of loops within the structure. It is plausible that the average size of single loops within the structure resulting from loop interaction and agglomeration, and with this perhaps also the size of the denuded zone close to the dislocation ('stand-off distance') will increase with temperature. At constant interstitial content, the loop density would decrease correspondingly.

In the high temperature region, the decoration phenomenon is most likely to be limited by the enhanced loop absorption by dislocations due to increasingly faster BV changes and/or climb with increasing temperature. At the low temperature side, the effect is probably not limited by the freezing-in of the migration of small glissile loops, as one might expect, but rather by the rapid increase in the cluster density between the dislocations which causes a rapid decrease in the mean free path λ before the structure would have a chance to evolve.

The temperature dependence of λ is also responsible for the temperature dependence of the 'incubation dose' introduced in Eq. (20). Thus, $G\tau_i$ is estimated in pure Cu to change from an extremely low value of about 5×10^{-5} dpa at 523 K where $\lambda \geq 20$ μm to about 5×10^{-3} dpa at around room temperature where $\lambda \approx 200$ nm. These values appear to be consistent with microstructural observations on pure Cu. Any delay in the accumulation of loops near dislocations to doses above the value given by Eq. (20) may be considered to be due to a (weak) violation of Eq. (21).

The evolution of a dense structure of loops in the form of a dislocation wall may be considered as a fractal dislocation climb process. Neglecting real (perfect) climb of the original grow-in dislocation by SIA loop absorption and assuming that strong loop trapping and mutual immobilization occurs in a strip of width $d \approx 20$ nm ahead of the existing saturated structure we may write the growth velocity as

$$v = \varepsilon_i^g P d \lambda(t)/\alpha b, \tag{22}$$

where $\alpha \approx 0.5$ is now the saturation value of the covered areal fraction of the wall. Estimating the average value of $\lambda(t)$ for Cu irradiated with neutrons at 523 K to 10^{-2} dpa on the basis of microstructural data [16] to be about 5 μm and assuming as above $G = 10^{-7}$/s and $\varepsilon_i^g = 5\%$ we obtain from Eq. (22) a wall width of about 0.4 μm consistent with the experimental observation shown in Fig. 2 [28]. This agreement confirms our assumption that a possible climb of the original dislocation by loop absorption which would reduce the wall width may be neglected in this case indicating that Eq. (21) is fulfilled under these conditions. The situation may, however, qualitatively change at higher dose where wall growth is expected to slow down because of decreasing $\lambda(t)$ and the structure may be eaten up from behind by climb of the original dislocation (fourth phase in Fig. 10).

3. Radiation hardening under cascade damage conditions

There is now clear evidence for a strong correlation between the cascade induced decoration of dislocations with SIA clusters and the mechanical behaviour of metals and alloys as has been documented recently [28,41]. Before discussing this correlation in some detail, we briefly summarize the main experimental results obtained in post-irradiation tensile tests [41].

3.1. Experimental results

In order to identify the role of irradiation-induced defects in modifying the deformation behaviour of irradiated metals and alloys it is useful to distinguish between initiation (yielding) and continuation (work hardening or softening) stages of the plastic flow:

(1) Initiation:

(a) The yield stress increases with irradiation dose to which the sample was exposed and this increase appears to occur without the generation of dislocations.

(b) Beyond a certain dose level, a pronounced yield drop is observed.

(c) The threshold dose for the occurrence of a yield drop depends on the pre-irradiation microstructure: it is low for well annealed pure metals characterized by a low density of grown-in dislocations (≈ 0.01 dpa in Cu) and seems to increase, for alloys, with the complexity of the structure; a dispersion of precipitates may prevent the occurrence of a yield drop (e.g., Y_2O_3 particles in Zr).

(d) The threshold dose seems to decrease with increasing temperature. No yield drop is observed at the high temperature side of the decoration phenomenon inspite of

the occurrence of well pronounced loop structures near dislocations in that temperature range ($\sim 0.4T_m$ in fcc).

(2) Continuation:

(a) Beyond the yield drop, plastic instability rather than work hardening is observed in many cases.

(b) In such cases, narrow bands representing only a small fraction of the sample volume have been found to be virtually cleared from defect clusters in post-irradiation/post-test microstructural investigations, indicating that plastic deformation is localized in these bands.

(c) The details of the plastic deformation behaviour (work hardening or softening) depends, similar to the yield drop on the initial mirostructure (for instance work hardening in Cu single crystals but not in polycrystalline Cu).

3.2. Modeling

Radiation hardening under cascade damage conditions and its modeling has been reanalysed recently [41]. In the following, the main points of the analysis are briefly summarized.

There are two distinctly different mechanisms for primary hardening (increase in the yield stress) of unirradiated metallic systems corresponding to two extreme microstructural situations: (1) hardening due to an essentially homogeneous dispersion of precipitate particles (precipitate hardening, dispersed barrier hardening, DBH [42–44]), and (2) hardening due to a localized enhancement of impurity concentrations along dislocations (source hardening, SH [46]).

In the first case, dispersed particles act as (in the extreme case impenetrable, indestructible) obstacles against the gliding of dislocations and the yield stress is defined, according to Orowan [42–44], by the resolved shear stress necessary for a dislocation to overcome the obstacles by bowing out between them. Upon yielding, dislocation segments pinned at two sides may act as Frank–Read sources for creation of dislocations. Hence, in this case, the initiation of plastic flow is characterized by the creation of new dislocations. The interaction between an increasing number of dislocations may result in work hardening.

In the second case, the dislocations are locked by clouds of impurities and the (upper) yield stress is defined, according to Cottrell [46], by the resolved shear stress required to pull the dislocations away from their impurity 'atmosphere'. The transition from locked to free dislocations manifests itself in a yield drop.

Attempts have been made to apply both types of hardening models to radiation hardening. Thus, Seeger's zone theory of radiation hardening [45] in which cascade induced vacancy clusters are assumed to act as barriers to gliding dislocations is essentially an application of Orowan's model. In such models of radiation hardening, a parameter for characterizing the 'strength' of defect clusters is commonly introduced — mainly to fit the experimental data. Striking features in radiation hardening such as the increase in the yield stress without dislocation generation, the yield drop, the tendency to plastic instability and the localization of plastic flow to narrow bands can, however, not be rationalized in terms of this model. The lack of clusters within deformation channels clearly shows that such clusters do not form obstacles against gliding dislocations (even no 'soft' obstacles) but are absorbed by the dislocations.

Previous attempts to describe radiation hardening in terms of 'defect cloud' formation along grown-in dislocations [47–49] correspond to Cottrell's model of solution hardening [46]. The character and origin of the defects forming these clouds were, however, not known in these early attempts.

Recently, radiation hardening under cascade damage conditions has been treated in terms of cascade induced source hardening (CISH) [41] where the defect structure locking the dislocations is assumed to originate from the glide and trapping of cascade induced glissile SIA loops as discussed in Section 2. This model is able to fully account for the deformation characteristics described above. Thus, the upper yield stress appearing above some critical dose may be related to the break-away stress which is necessary to pull the dislocations away from the loops decorating them. The yield drop and plastic instability may be attributed to the localization of deformation in the form of cleared channels resulting from the sweeping away of isolated clusters by moving dislocations. The initial microstructure may affect the deformation behaviour directly by enhancing hardening, or indirectly by influencing the evolution of the decoration process. In alloys, the source hardening due to dislocation decoration may get rather complicated by the possibility of impurity segregation either directly on the dislocation or on the SIA loops decorating them. However, regardless of these complications, the CISH mechanism would principally operate even in alloys.

3.3. Relation between microstructure and upper yield stress

In order to assess the relation between the microstructural characteristics of a loop ensemble decorating a dislocation and the stress necessary to unlock the dislocation from the loop ensemble we consider two idealized situations as sketched in Fig. 12. (a) The loops are clearly separated by distances similar to their size (a row of loops), and (b) the loops are no longer well separated but form a network in which they have, at least partly, lost their individuality.

In the first case, we may neglect the effect of dislocation bowing out between neighbouring loops. For this case, we consider a straight row of sessile edge type loops of Burgers vector, b, diameter d, and spacing l at a distance y (stand-off distance) parallel to a straight glissile edge dislocation of Burgers vector, b, in an elastically isotropic medium of shear modulus μ and Poisson's ratio ν. Using

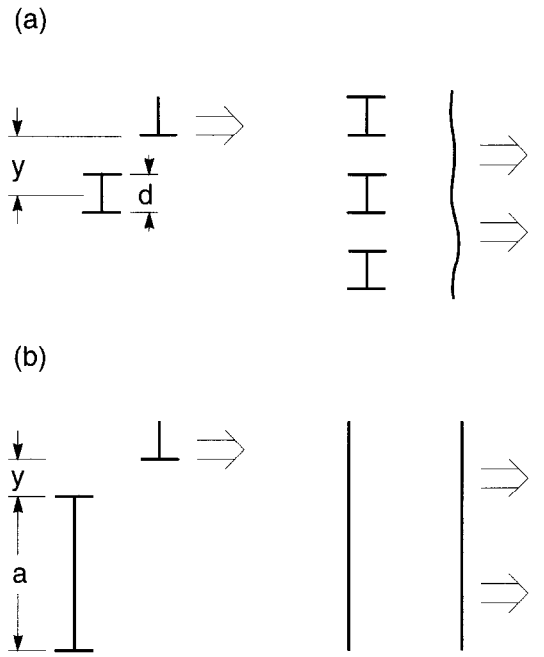

Fig. 12. Schematic illustration of the unlocking of a dislocation from (a) a row of loops, (b) a loop ensemble approximated by a dislocation dipole; cross-sectional view (left) and projection on glide plane (right).

the infinitesimal loop approximation we find that the force acting between one loop and the dislocation is maximum ($\partial E^2/\partial x^2 = 0$) at an angle of about 40° between the distance vector and the glide plane of the dislocation where it assumes a value

$$F_{dl} \approx 0.069(\mu/(1-\nu))(bd/y)^2. \tag{23a}$$

This force must be compensated by the force on the dislocation due to the external shear stress $\tilde{\sigma}$ (resolved shear stress)

$$F_{\sigma d} = \tilde{\sigma} bl. \tag{23b}$$

The condition $F_{dl} = F_{\sigma d}$ yields for the stress necessary to unlock the dislocation (at $\nu = 1/3$)

$$\tilde{\sigma} \cong 0.1\mu(b/l)(d/y)^2. \tag{24}$$

According to Eq. (24), an upper yield stress of the order of 300 MPa for copper irradiated with neutrons at ≈ 320 K [28] (directional average of $\mu = 55$ GPa) would be consistent with $(b/l)(d/y)^2 \cong 5 \times 10^{-2}$ obtained, for instance, by taking $l = 35b$ (≈ 10 nm) and $y = 0.75d$ which are quite reasonable in view of the observed microstructure [28]. The presence of loops with Burgers vectors different from that of the lead dislocation would require lower values of l and y to yield the same upper yield stress of 300 MPa.

For the second case, we approximate the loop ensemble accumulated near the dislocation by a sessile dislocation dipole of Burgers vector, b', and diameter, a, separated from the leading dislocation by a stand-off distance y. For $a \gg y$, holding for a well developed loop structure, the externally applied shear stress has to overcome the maximum attractive shear stress exerted by the close dislocation component of the dipole on the primary dislocation occurring at 22.5° between the distance vector and the glide plane. For $b' = b$, the corresponding condition yields an estimate for the upper yield stress given by

$$\tilde{\sigma} \approx Gb/8\pi(1-\nu)y. \tag{25}$$

According to Eq. (25), an upper yield stress of the order of 300 MPa for copper irradiated with neutrons at ≈ 320 K would be consistent with $y = 10b$ (≈ 25 nm). This would suggest that in this case the stand-off distance, y, is only of the order of a few nanometers which is in a reasonable agreement with the observed spatial distribution of loops in the vicinity of decorated dislocations. A lateral smearing out of the dislocation dipole representing the loop ensemble would require lower values of y. It should be noticed that the meaning of y is somewhat different here than in the first case because of a different geometry. Independent of precise details, our estimates show that the locking mechanism proposed in the present paper provides a possible explanation for the observed radiation hardening.

3.4. Dose and temperature dependencies of radiation hardening

The dose and temperature dependencies of radiation hardening are closely related to those of the underlying microstructure. Sections 2.5 and 3.3 form therefore the basis for the following discussion. The increase in the yield stress with dose without the generation of dislocations may be considered to be due to an increasingly stronger locking of dislocations by continuously accumulating loops in their vicinity. Our model is, however, not yet sufficiently detailed to describe the dose dependence of the yield stress quantitatively. As discussed in the previous section, within the framework of the CISH model, the main parameters controlling the upper yield stress are the stand-off distance, y, the inter-loop spacing, l, and the loop diameter, d.

At lower temperatures, the stand-off distance is not expected to change much with the irradiation dose. On the other hand, the loop spacing will decrease due to continuous loop accumulation whereas the loop size will increase due to loop agglomeration with increasing dose. The details in the evolution of the decoration process depend on the flux of glissile loops to the decoration region which decreases with the build up of defect clusters in the regions between the dislocations and reaches a minimum value when the defect cluster density between the dislocations

reach a quasi-steady-state level. This would suggest that, at least qualitatively, the yield stress would increase with increasing dose and would come to saturate at a certain dose level. However, at present, the degree of loop accumulation causing maximum increase in the upper yield stress is not known. Work is in progress to quantify these aspects of the dose dependence.

For undelayed and pronounced accumulation of loops near dislocations, as developing in pure metals such as Cu, the threshold dose for the appearance of a yield drop is expected to correspond to the dose of mutual loop immobilization as given by Eq. (20). In fact, the value of 5×10^{-3} dpa estimated above for Cu irradiated around room temperature agrees well with the dose at which a yield drop is observed to occur in Cu single crystals [38]. At 523 K, the dose estimated according to Eq. (20) would be two orders of magnitude lower. At this temperature, however, no yield drop at all is observed inspite of the occurrence of well developed loop structures near dislocations.

The deformation characteristics of CISH is expected to disappear at the low and high temperature limits of the dislocation/loop decoration phenomenon, i.e., at about 0.15 and $0.4T_m$ because of decreasing loop supply regions and enhanced loop absorption, respectively. In order to understand the temperature dependence of the upper yield stress and the yield drop, we consider the relation between the loop structure and the upper yield stress as discussed in the preceding section. According to Eqs. (24) and (25), the upper yield stress is expected to become temperature dependent via the diameter d of the loops, their spacing l, and the stand-off distance y. Even though the detailed temperature dependence of these quantities is not known presently the qualitative trends are quite clear. Thus, d, l and y may be expected to increase and accordingly $\tilde{\sigma}$ to decrease with increasing temperature. Close to the high temperature limit of the decoration phenomenon, the shear stress necessary to unlock a dislocation from the loop structure decorating it is likely to be at such a low level (below 100 MPa) that source hardening is masked by barrier and work hardening.

4. Summary and conclusions

Many microstructural studies of metals and alloys subjected to cascade damage have revealed a pronounced segregation of small dislocation loops of SIA type in the vicinity of grown-in dislocations. Post-irradiation tensile tests performed on such materials exhibit the typical features of source hardening characterized by an increased yield stress without dislocation generation, a tendency to plastic instability beyond the yield drop and a pronounced localization of the plastic flow in narrow bands. In the present paper, possible mechanisms for the accumulation of SIA loops near dislocations and the correlation of this effect with the deformation characteristics have been discussed. The main conclusions may be summarized as follows.

(1) Decoration of dislocations with SIA loops:

(a) It has been shown that this phenomenon cannot be rationalized in terms of enhanced agglomeration of single three-dimensionally migrating SIAs in the strain field of a dislocation since this induces a depletion not only in the compressive but also in the dilatational region resulting in reduced rather than enhanced agglomeration of SIAs. SIA depletion, particularly at the compressive side, may, however, induce enhanced vacancy agglomeration as has been occasionally observed after electron irradiation.

(b) Our analysis suggests that the trapping and accumulation of SIAs near dislocations would require a restriction of the dimension of the SIA migration which is most efficient for the case of a strictly one-dimensional motion. Any transversal component in the motion by conservative climb or a discrete change in the migration direction by Burgers vector change must be relatively small or rare, respectively, to ensure efficient SIA accumulation. A possible metastable one-dimensionally migrating crowdion configuration is highly unlikely to fulfill this requirement. Groups of crowdions in the form of glissile perfect SIA loops, on the other hand, could do this. We, therefore, consider the decoration phenomenon to be due to the glide and trapping of glissile SIA loops directly produced in cascades.

(c) Small loops trapped in the strain field of a dislocation may be detrapped by thermal activation or approach the dislocation by thermally activated changes in the Burgers vector and/or by conservative climb. Decoration of dislocations with loops requires that a single trapped loop is immobilized by other loops before it is detrapped from or absorbed by the dislocation. This requirement imposes conditions on the relative rates of detrapping, Burgers vector change, climb and immobilization which have been discussed. A loop migration mechanism accounting for these conditions has been suggested.

(d) The dose dependence of the decoration phenomenon is characterized by early stages in which the loop structure reaches a relative stability by mutual loop immobilization followed by later stages in which a saturated loop structure grows. The wide temperature range (0.15 to $0.4T_m$) may be explained by a broad spectrum of cascade induced SIA cluster sizes and a correspondingly broad spectrum of activation energies for glide and Burgers vector changes.

(2) Radiation hardening:

(a) The deformation characteristic of metals and alloys subjected to cascade damage conditions (increase in yield stress without dislocation generation, yield drop, plastic instability, localization of plastic flow) cannot be rationalized in terms of conventional dispersed barrier hardening but may be described in terms of cascade induced source hardening (CISH) where the dislocations are considered to

be locked by the loops decorating them. The removal of defect clusters from bands where plastic flow is localized after the unlocking of dislocations under a sufficiently high stress clearly demonstrates that such clusters do not form different obstacles against dislocation glide but are swept and absorbed by dislocations.

(b) The relation between the structure of the loop accumulation and the upper yield stress has been discussed. Apart from the loop size and the distance between the loops in the decorated region, a key parameter of the structure is the stand-off distance. The parameter sets required to explain the observed levels of the yield stress appear reasonable.

(c) The dose and temperature dependence of radiation hardening is closely related to that of the underlying loop accumulation. The dose for the appearance of a yield drop seems to be correlated with the dose required for mutual immobilization of loops trapped near dislocations. The temperature dependence of the upper yield stress may be considered to be due to that of the loop structure. With increasing temperature, the structure becomes coarser and the yield stress decreases correspondingly, and this eventually to a low level where source hardening becomes inefficient.

References

[1] H. Trinkaus, B.N. Singh, A.J.E. Foreman, J. Nucl. Mater. 206 (1993) 200.
[2] H. Trinkaus, B.N. Singh, C.H. Woo, J. Nucl. Mater. 212–215 (1994) 18.
[3] B.N. Singh, S.I. Golubov, H. Trinkaus, A. Serra, Yu.N. Osetsky, A.V. Barashev, these Proceedings, p. 107.
[4] T. Diaz de la Rubia, M.W. Guinan, J. Nucl. Mater. 174 (1990) 151.
[5] T. Diaz de la Rubia, M.W. Guinan, Phys. Rev. Lett. 66 (1991) 2766.
[6] A.J.E. Foreman, C.A. English, W.J. Phythian, Philos. Mag. A66 (1992) 655.
[7] A.J.E. Foreman, C.A. English, W.J. Phythian, Philos. Mag. A66 (1992) 671.
[8] C.H. Woo, B.N. Singh, Phys. Status Solidi B159 (1990) 609.
[9] C.H. Woo, B.N. Singh, Philos. Mag. A65 (1992) 889.
[10] A.D. Brailsford, R. Bullough, Philos. Trans. Roy. Soc. (London) 302 (1981) 87.
[11] T. Leffers, B.N. Singh, A.V. Volobuyev, V.V. Gann, Philos. Mag. A53 (1986) 243.
[12] B.N. Singh, T. Leffers, A. Horsewell, Philos. Mag. A53 (1996) 233.
[13] J.O. Stiegler, E.E. Bloom, Radiat. Eff. 8 (1971) 33.
[14] B.N. Singh, T. Leffers, W.V. Green, S.L. Green, J. Nucl. Mater. 105 (1982) 1.
[15] A. Horsewell, B.N. Singh, ASTM-STP 955 (1988) 220.
[16] B.N. Singh, S.J. Zinkle, J. Nucl. Mater. 206 (1993) 212.
[17] J.L. Brimhall, B. Mastel, Radiat. Eff. 3 (1970) 203.
[18] V.K. Sikka, J. Moteff, J. Nucl. Mater. 54 (1974) 325.
[19] J. Bentley, B.L. Eyre, M.H. Loretto, US-ERDA Conf. 751006, Gatlinburg, 1975, p. 925.
[20] J.H. Evans, J. Nucl. Mater. 88 (1980) 31.
[21] K. Yamakawa, Y. Shimomura, J. Nucl. Mater. 155–157 (1988) 1211.
[22] B.N. Singh, J.H. Evans, A. Horsewell, P. Toft, D.J. Edwards, J. Nucl. Mater. 223 (1995) 95.
[23] B.N. Singh, J.H. Evans, to be published.
[24] M. Kiritani, Mater. Sci. Forum 15–18 (1987) 1023.
[25] S. Kojima, T. Yoshiie, M. Kiritani, J. Nucl. Mater. 155–157 (1988) 1249.
[26] Y. Satoh, I. Ishida, T. Yoshiie, M. Kiritani, J. Nucl. Mater. 155–157 (1988) 443.
[27] M. Kiritani, private communication.
[28] B.N. Singh, A. Horsewell, P. Toft, D.J. Edwards, J. Nucl. Mater. 224 (1995) 131.
[29] B.C. Larsen, F.W. Young, in: Radiation Induced Voids in Metals, Proc. Albany Conf., USAEC Symp. Services 26, CONF-710601, eds. J.W. Corbett and I.C. Ianniello (1971) p. 672.
[30] C.A. English, B.L. Eyre, J.W. Muncie, Philos. Mag. A56 (1987) 453.
[31] M. Suehiro, N. Yoshida, M. Kiritani, Proc. Yamada Conf. V, Point Defects and Defect Interactions in Metals (University of Tokyo Press, 1982).
[32] W. Sigle, M.L. Jenkins, J.L. Hutchison, Philos. Mag. Lett. 57 (1988) 267.
[33] S.L. King, M.L. Jenkins, M.A. Kirk, C.A. English, J. Nucl. Mater. 205 (1993) 467.
[34] B.N. Singh, M.R. Warren, P.D. Parson, in: Nuclear Fuel Performance, Proc. Int. Conf., Br. Nuclear Energy Soc., 15–19 Oct. 1973, London, eds. C.T. John, B. Wyles and B. Moore (BNES, London, 1973) p. 64.1.
[35] M.I. de Vries, in: ECN (Petten) Rept. ECN-C-90-041, Aug. 1990, ed. J.G. van der Laan, p. 66.
[36] G.V. Müller, D. Vavillet, M. Victoria, J.L. Martin, J. Nucl. Mater. 212–215 (1994) 1283.
[37] B.N. Singh, A. Horsewell, P. Toft, J.H. Evans, J. Nucl. Mater. 212 (1994) 1292.
[38] Y. Dai, PhD thesis (No. 1388), University of Lausanne (1995) p. 59.
[39] M.J. Makin, Philos. Mag. 10 (1994) 695.
[40] H. Trinkaus, B.N. Singh, A.J.E. Foreman, J. Nucl. Mater. 249 (1997) 91.
[41] B.N. Singh, A.J.E. Foreman, H. Trinkaus, J. Nucl. Mater. 249 (1997) 103.
[42] E. Orowan, Nature 149 (1942) 643.
[43] E. Orowan, Symp. Int. Stresses in Metals and Alloys (Institute of Metals, London, 1948) p. 451.
[44] E. Orowan, Dislocations in Metals (AIME, New York, 1954) p. 131.
[45] A. Seeger, Proc. 2nd UN Int. Conf. on Peaceful Uses of Atomic Energy, Geneva, Sept. 1958, Vol. 6, p. 250.
[46] A.H. Cottrell, Dislocations and Plastic Flow in Crystals (Clarendon Press, Oxford, 1953).
[47] T.H. Blewitt, R.R. Coltman, R.E. Jamison, J.K. Redman, J. Nucl. Mater. 2 (1960) 277.
[48] F.W. Young, J. Appl. Phys. 33 (1962) 3553.
[49] D.K. Holmes, The Interaction of Radiation with Solids (North-Holland, Amsterdam, 1964) p. 147.

[50] F. Kroupa, in: Theory of Crystal Defects, ed. Gruber (Academic Press, New York, 1966).
[51] P. Ehrhart, K.H. Robrock, H.R. Schober, in: Physics of Radiation Effects in Crystals, eds. R.A. Johnson and A.N. Orlov (Elsevier, Amsterdam, 1986).
[52] P.H. Dederichs, K. Schroeder, Phys. Rev. B17 (1978) 2524.
[53] F.S. Ham, J. Appl. Phys. 30 (1959) 915.
[54] I.G. Margvelashvili, Z.K. Saralidze, Sov. Phys. Solid State 15 (1974) 1774.
[55] B.L. Eyre, D.M. Maher, Philos. Mag. 24 (1971) 767.